# Critical behavior of an array of Josephson junctions with variable couplings

H. Eikmans and J. E. van Himbergen
*Institute for Theoretical Physics, Princetonplein 5, P.O. Box 80.006, 3508 TA Utrecht, The Netherlands*

H. J. F. Knops and J. M. Thijssen
*Institute for Theoretical Physics, University of Nijmegen, Toernooiveld, 6525 ED Nijmegen, The Netherlands*
(Received 7 December 1988)

We consider a generalization of the fully frustrated $XY$ model in two dimensions, introduced by Berge *et al.* We derive the Coulomb gas representation of the partition function. From the form of the interaction between half-integer charges we infer that, away from full frustration, dipoles are formed out of neighboring charges and that the low-temperature phase transition is an Ising transition in this system of dipoles. The charges which are not bound in dipoles fuse in pairs to form a dilute gas of integer charges. The transition in this gas is a normal Kosterlitz-Thouless transition and is not triggered by the Ising transition. In fact, we make it plausible that the transitions only coincide at full frustration. Our picture is supported by Monte Carlo simulations.

## I. INTRODUCTION

In recent years experimental interest in arrays of superconducting islands coupled by Josephson junctions has greatly stimulated theoretical work on frustrated classical two-dimensional (2D) $XY$ models in an effort to understand the critical behavior of such arrays.[1] One of the most interesting features of these models is the simultaneous occurrence of domain walls and vortex excitations. The former are due to discrete symmetry (introduced by degeneracy of the ground state as a result of frustration), the latter to the continuous symmetry of spin (i.e., phase of the superconducting order parameter) rotation. Despite much theoretical progress (see e.g., Ref. 1), our insight into the critical behavior of such systems is far from complete; in particular, the role played by domain walls in the dissociation of vortex-antivortex pairs is not well understood.

Very recently two different experimental techniques, dynamic response to small oscillating fields[2] and voltage noise measurements,[3] have yielded what appears to be the first direct evidence of domain-wall excitations in Josephson junction arrays. Since this opens prospects for more definitive comparison between theory and experiment, we have taken a new look at a frustrated $XY$ model introduced some time ago by Berge *et al.*[4] The attractive feature of this model is that it describes an array with variable degree of frustration that can actually be built by varying the surface area of selected junctions in the array.[5]

The model is described by the Hamiltonian

$$H=-\sum_{\langle \mathbf{r},\mathbf{r}'\rangle} |J_{\mathbf{r}\mathbf{r}'}|\cos[\theta(\mathbf{r})-\theta(\mathbf{r}')-2\pi A(\mathbf{r},\mathbf{r}')] \tag{1.1}$$

with nearest-neighbor coupling between classical spins $\theta(\mathbf{r})$ on a square lattice. Each square has three ferromagnetic bonds $J$ and one bond of variable strength $-\eta J$ as depicted in Fig. 1.[4] If $\eta>0$ we will take the bond strength to be $+\eta J$ and absorb the sign in the argument of the cosine by taking

$$A(\mathbf{r},\mathbf{r}')=\begin{cases}\frac{1}{2} \text{ on } \eta \text{ bonds}, \\ 0 \text{ otherwise}.\end{cases} \tag{1.2}$$

Of course, $A(\mathbf{r},\mathbf{r}')=0$ for all bonds if $\eta<0$. For $\eta=1$, this model is a realization of the fully frustrated $XY$ model with a doubly degenerate ground state (see, e.g., Ref. 6). For all $\eta>\eta_c=\frac{1}{3}$, a doubly degenerate ground state of canted spins exists, and, hence, domain walls. As $\eta$ changes one expects domain-wall energies to vary with respect to the strength of the vortex-pair potential. For $\eta<\eta_c$ the ground state is ferromagnetic; for $\eta=-1$ the model corresponds to an isotropic ferromagnet. In the following we will use the terms strong and weak horizontal bonds to indicate the bonds with the largest and smallest value of $|J_{\mathbf{r}\mathbf{r}'}|$, respectively.

In contrast with the fully frustrated case $\eta=1$ (Ref. 6–8), few results exist for this model at $\eta\neq 1$. Monte Carlo (MC) simulations[4] support a phase-transition scenario in which an Ising-like transition (due to the proliferation of domain walls) takes place at a lower temperature than the Kosterlitz-Thouless (KT) transition (associated with vortex-antivortex pair dissociation). A similar scenario is observed for coupled $XY$ models.[9] The fact that the KT transition, in these models, occurs after the Ising transition, i.e., in the Ising *disordered* phase, is in sharp contrast with the observed behavior for homogeneous (frustrated) models.[6–8,10,12] It was argued[7,11,12] that the presence of fractional charges, which become free by the melting of domain walls at the Ising transition, directly triggers the KT transition. In this paper we want to show how this picture is altered for the $\eta\neq 1$ systems so that the Ising and KT transition can occur in the reverse order. A theoretical analysis of the $\eta\neq 1$ systems has also recently be given by Granato and Kosterlitz.[13] However, these authors start from a Landau-Ginzburg approximation for the frustrated $XY$ model. In this approximation the fractional charges are no longer present,

 

so that no insight can be gained why the homogeneous models behave so differently from the inhomogeneous ones. In fact, the Landau-Ginzburg picture *always* favors the scenario where the Ising transition precedes the KT transition at increasing temperature.[9]

## II. THE COULOMB GAS

In this section we will write the partition function of the model as a grand canonical partition function $Z_{CG}$ of a 2D Coulomb gas (CG). The form of $Z_{CG}$ is

$$Z_{CG}=\sum_{\{M\}}\exp(-H_{CG}/T)\ , \tag{2.1a}$$

where the Coulomb gas Hamiltonian $H_{CG}$ can be written as

$$H_{CG}=2\pi^2\tilde{J}\sum_{\mathbf{R},\mathbf{R}'}M(\mathbf{R})G(\mathbf{R},\mathbf{R}')M(\mathbf{R}')\ . \tag{2.1b}$$

The variables $M(\mathbf{R})$, which represent the local vorticity, are integer charges or half-integer charges depending on $\eta$. $\mathbf{R}$ and $\mathbf{R}'$ denote sites on the dual lattice and the summation in (2.1a) is over all neutral charge configurations. The function to be determined is the lattice Green's function $G(\mathbf{R},\mathbf{R}')$. As a first step in our search for $G$ we replace (1.1) by its periodic Gaussian (PG) form. We then obtain the Hamiltonian

$$H_{PG}(\{\varphi(\mathbf{r})\},\{m(\mathbf{r},\mathbf{r}')\})=\sum_{\langle\mathbf{r},\mathbf{r}'\rangle}\frac{|\tilde{J}_{\mathbf{r}\mathbf{r}'}|}{2}\{\varphi(\mathbf{r})-\varphi(\mathbf{r}')-2\pi[m(\mathbf{r},\mathbf{r}')+\tilde{A}(\mathbf{r},\mathbf{r}')]\}^2 \tag{2.2}$$

with new degrees of freedom $\{\varphi(\mathbf{r})\}$ and $\{m(\mathbf{r},\mathbf{r}')\}$. The $\varphi(\mathbf{r})$'s are defined on $(-\infty,\infty)$. The $m(\mathbf{r},\mathbf{r}')$'s are integers and defined only on horizontal bonds.[14] As for the original model one takes $\tilde{J}_{\mathbf{r}\mathbf{r}'}$ to be either equal to $\tilde{J}$ or to $\tilde{\eta}\tilde{J}$. The value of $\tilde{J}$ can be used to tune the spin-wave stiffness of the PG model to that of the original model (e.g., for $\eta=1$ this would give $\tilde{J}=\frac{1}{2}\sqrt{2}J$, notice that the spin-wave excitations are to be taken with respect to the canted ground state). With the parameters $\tilde{\eta}$ and $\tilde{A}$ one can match the ground states of the two models. The PG model has a doubly degenerate ground state if we choose $\tilde{A}$ as in (1.2). Given (2.2) and (1.2) it is easy to see that the ground state will have either all $m(\mathbf{r},\mathbf{r}')=0$ or $m(\mathbf{r},\mathbf{r}')=-1$ for $\eta$ bonds and 0 otherwise (modulo an overall additive constant). The magnitudes of the phase differences are in both cases $3\pi\tilde{\eta}/(1+3\tilde{\eta})$ for $\eta$ bonds and $\pi\tilde{\eta}/(1+3\tilde{\eta})$ otherwise. Therefore, we conclude that $\eta_c=\frac{1}{3}$ corresponds to $\tilde{\eta}=0$, while, of course, the analog of $\eta=1$ is obtained by taking $|\tilde{\eta}|=1$ and $\tilde{A}$ as in (1.2). The precise relationship $\tilde{J}(J,\eta)$ and $\tilde{\eta}(\eta)$ does not concern us here as we are mainly interested in explaining the topology of the phase diagram (the inverted order of the Ising and KT transitions and their critical behavior). Henceforth, we will simply denote $\tilde{\eta}$ and $\tilde{J}$ by $\eta$ and $J$, respectively, and we will only deal with choice (1.2) for $\tilde{A}$.

Next, application of a few well-known steps[14] gives us the inverse-lattice Green's function

$$\begin{aligned}G^{-1}(\mathbf{R},\mathbf{R}'')=&(2\delta_{\mathbf{R}'',\mathbf{R}}-\delta_{\mathbf{R}'',\mathbf{R}+\hat{e}_1}-\delta_{\mathbf{R}'',\mathbf{R}-\hat{e}_1})\\&+a(\delta_{\mathbf{R}'',\mathbf{R}}-\delta_{\mathbf{R}'',\mathbf{R}+\hat{e}_2})\\&+b(\delta_{\mathbf{R}'',\mathbf{R}}-\delta_{\mathbf{R}'',\mathbf{R}-\hat{e}_2})\ .\end{aligned} \tag{2.3}$$

The coordinate axes are shown in Fig. 1. $\mathbf{R}$ and $\mathbf{R}''$ are sites on lattice 1 or 2 as defined in Fig. 1. The origin is taken to lie on lattice 1. $a=1$, $b=|\eta|^{-1}$ if $\mathbf{R}$ is on 1, and $a=|\eta|^{-1}$, $b=1$ if $\mathbf{R}$ is on 2. The lattice Green's function $G$ is defined through

$$\sum_{\mathbf{R}''}G^{-1}(\mathbf{R},\mathbf{R}'')G(\mathbf{R}'',\mathbf{R}')=\delta_{\mathbf{R},\mathbf{R}'}\ . \tag{2.4}$$

One readily recognizes that for $|\eta|=1$ the usual discrete Poisson equation is recovered. The resulting Green's function in this case is the (discrete) Coulomb potential acting between charges located at the dual lattice sites. We now want to see how this picture alters for $\eta\neq1$.

We can solve (2.4) for $G$ by performing a Fourier transform. In this way we obtain an exact expression for the (Fourier transform of) $G$. This method is discussed in the Appendix. The derivation presented here is not exact but it is transparent and directly gives a clear intuitive picture of the resulting Coulomb gas. We start with the following observation: if $\eta=0$ the Coulomb gas consists of integer charges. The asymptotic form of $G$ will be logarithmic when the charges are positioned at the centers of the double cells (indicated by the dot in Fig. 2). If $\eta=1$ we know that $G$ is asymptotically logarithmic when the charges are situated at the centers of the single cells (indicated by open circles). Therefore, we conjecture that at arbitrary $\eta$, $G$ can be made logarithmic if the charges are shifted to positions, somewhere on the dashed line (see Fig. 2). Hence, we try to find a solution of (2.4) of the form

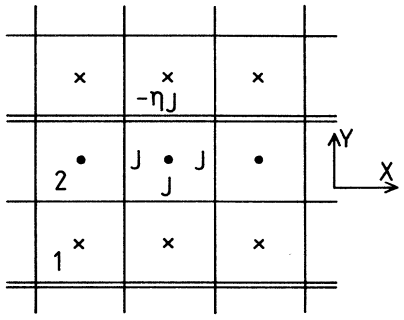


FIG. 1. A square lattice with alternating rows of bonds with variable strength as indicated. The dual lattice is divided into a lattice labeled 1 (crosses) and 2 (circles).

$$G(\mathbf{R},\mathbf{R}')=G_0[\mathbf{R}-\mathbf{R}'+2\delta(\mathbf{R},\mathbf{R}')\hat{\mathbf{e}}_y]\ , \tag{2.5a}$$

where

$$\delta(\mathbf{R},\mathbf{R}')=\begin{cases}-\delta \text{ if } \mathbf{R} \text{ is on 1 and } \mathbf{R}' \text{ on 2}\ ,\\ \delta \text{ if } \mathbf{R} \text{ is on 2 and } \mathbf{R}' \text{ on 1}\ ,\\ 0 \text{ if } \mathbf{R} \text{ and } \mathbf{R}' \text{ are on the same lattice}\ ,\end{cases} \tag{2.5b}$$

with $|\delta|\leq\frac{1}{2}$. (The lattice constant $a=1$.)

Now we seek a $\delta$ that makes $G_0$ asymptotically logarithmic. Strictly speaking, the lattice Green's function is defined only on the points of the dual lattice. Hence, we must specify what we mean by (2.5). A natural definition is in terms of a Taylor expansion

$$G_0(\mathbf{R}+\epsilon\hat{\mathbf{e}}_y)=\sum_{n=0}^{\infty}\epsilon^n\Delta_y^{(n)}G_0(\mathbf{R})\ . \tag{2.6}$$

Here $\Delta_y^{(n)}G_0$ is the discrete $n$th derivative of $G_0$ in the $y$ direction:

$$\begin{aligned}\Delta_y^{(1)}G_0(\mathbf{R})&\equiv\Delta_y G_0(\mathbf{R})\\ &=\tfrac{1}{2}[G_0(\mathbf{R}+\hat{\mathbf{e}}_y)-G_0(\mathbf{R}-\hat{\mathbf{e}}_y)]\ ,\\ \Delta_y^{(2)}G_0(\mathbf{R})&\equiv\Delta_{yy}G_0(\mathbf{R})\\ &=G_0(\mathbf{R}+\hat{\mathbf{e}}_y)+G_0(\mathbf{R}-\hat{\mathbf{e}}_y)-2G_0(\mathbf{R}),\ \text{etc.}\end{aligned} \tag{2.7}$$

We insert (2.5) in (2.4) and ignore all terms containing $\Delta_x^{(m)}G_0$ and $\Delta_y^{(m)}G_0$ with $m\geq 3$. Then we obtain four equations:

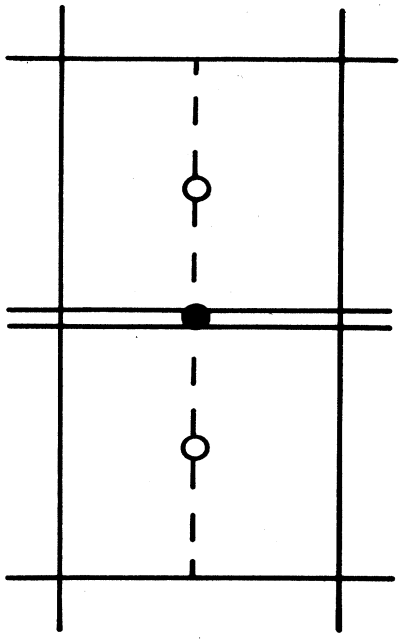

FIG. 2. A double cell with charge positions indicated for $\eta=0$ (the dot) and $|\eta|=1$ (open circles). For all other values of $|\eta|$ there are two charge positions which are situated on the dashed line, symmetrically around the $\eta$ bond.

$$\begin{aligned}&-\Delta_{xx}G_0(\mathbf{R})-\frac{1}{2}\left[\frac{1}{|\eta|}(1-2\delta)^2+(1+2\delta)^2\right]\Delta_{yy}G_0(\mathbf{R})\pm\left[\frac{1}{|\eta|}(1-2\delta)-(1+2\delta)\right]\Delta_y G_0(\mathbf{R})=\delta_{\mathbf{R},0}\ \text{ if } \mathbf{R} \text{ is on 1}\ ,\\ &-\Delta_{xx}G_0(\mathbf{R})-\frac{|\eta|+1}{2|\eta|}[1-(2\delta)^2]\Delta_{yy}G_0(R)\pm\left[\frac{1-|\eta|}{|\eta|}-\frac{1+|\eta|}{|\eta|}2\delta\right]\Delta_y G_0(\mathbf{R})=0\ \text{ if } \mathbf{R} \text{ is on 2}\ .\end{aligned} \tag{2.8}$$

These equations beautifully merge into

$$\left[\Delta_{xx}+\frac{2}{|\eta|+1}\Delta_{yy}\right]G_0(\mathbf{R})=-\delta_{\mathbf{R},0}\ \text{ for all } \mathbf{R} \tag{2.9a}$$

when one takes

$$\delta=\frac{1}{2}\left[\frac{1-|\eta|}{1+|\eta|}\right]\ . \tag{2.9b}$$

$G_0$ obeys an anisotropic version of the discrete Poisson equation. We can calculate the asymptotic form of $G_0$ in the usual manner[15] and find that

$$\begin{aligned}G_0'(\mathbf{R})&=G_0(0)-G_0(\mathbf{R})\\ &\cong\frac{\alpha}{2\pi}\left[\ln R_*+\gamma(\text{Euler})+\tfrac{1}{2}\ln\frac{32}{|\eta|+3}\right]\\ &\qquad\text{for } |\mathbf{R}|\gg 1\ ,\end{aligned} \tag{2.10}$$

where

$$\alpha=\left[\frac{|\eta|+1}{2}\right]^{1/2}$$

and

$$R_*^2=R_x^2+\alpha^2R_y^2\ .$$

The Coulomb gas Hamiltonian now reads

$$H_{\mathrm{CG}}=-2\pi^2J\sum_{\mathbf{R}\neq\mathbf{R}'}M(\mathbf{R})\times G_0'[\mathbf{R}-\mathbf{R}'+2\delta(\mathbf{R},\mathbf{R}')\hat{\mathbf{e}}_y]M(\mathbf{R}')\ . \tag{2.11}$$

With (2.11) an intuitive picture arises: If $|\eta-1|$ increases, then the charges approach each other more and more on either side of the weak horizontal bonds. In this way dipoles are formed. Now it is convenient to represent the charge distribution by variables located at the centers of the weak bonds; one defines a net charge by

$$m(\mathbf{r})=M\left[\mathbf{r}+\frac{\hat{\mathbf{e}}_y}{2}\right]+M\left[\mathbf{r}-\frac{\hat{\mathbf{e}}_y}{2}\right] \tag{2.12a}$$

and a dipole moment by

$$\mathbf{p}(\mathbf{r})=(1-2\delta)\tfrac{1}{2}s(\mathbf{r})\hat{\mathbf{e}}_y=\frac{|\eta|}{|\eta|+1}s(\mathbf{r})\hat{\mathbf{e}}_y\ , \tag{2.12b}$$

where the "spin" $s(\mathbf{r})$ is defined by

$$s(\mathbf{r})=M\left[\mathbf{r}+\frac{\hat{\mathbf{e}}_y}{2}\right]-M\left[\mathbf{r}-\frac{\hat{\mathbf{e}}_y}{2}\right]\ . \tag{2.12c}$$

It is clear that with this definition the ground state has $m(\mathbf{r})\equiv 0$ and alternating columns with all $s(\mathbf{r})$ either $+1$ or $-1$. In order to understand the topology of the phase diagram one has to consider the excitations out of this ground state. In the case $\eta=1$ it turned out[11] to be useful to picture these excitations as domain walls on the bonds of the original lattice, separating the two possible ground-state charge configurations. It was shown that all charges effectively average out except for the corners of the domain walls where fractional charges appear. When the system is in the Ising ordered phase the domain walls are short and form small islands with a net charge (due to the fractional charges at all corners) that is *integer*. It is these integer charges that can exhibit a KT transition to a phase where the Coulomb potential is screened to a Debye-Hückel form. The transition point is given by the formula

$$T_{\mathrm{KT}}=\frac{\pi}{2}J_r e^2\ , \tag{2.13}$$

where $J_r$ is the renormalized Coulomb coupling and $e$ is the elementary free charge, which is $e=\pm 1$ in the Ising ordered phase. However, as soon as the Ising transition takes place the domain walls melt and large domains can occur. This means that there are now free fractional charges present. Since these charges screen the Coulomb potential already at a much lower temperature [see (2.13)], the Ising transition will directly trigger the KT transition. The conclusion is that on raising the temperature one should have either a KT transition that precedes an Ising transition, or a joint Ising-KT transition line. This conclusion is confirmed by numerical simulations.[12]

Now we consider the case $\eta\neq 1$. It is evident from our picture of shifted charges that the energy of a wall on a weak bond is larger than that on a strong bond. To make this statement more quantitative we calculated the energy per unit length of infinite straight domain walls. In the Appendix we give the exact expressions for walls on the two types of horizontal bonds and for vertical walls. The resulting quantities are plotted in Fig. 3 as a function of $\eta$. We see that when $|\eta-1|$ is not too small then there is a substantial difference in energy between the two types of horizontal domain walls. (The energy of walls on $\eta$ bonds is, of course, finite at $\eta=0$.)

In our representation of the charges (2.12) a wall on a strong bond will induce a change in the polarization $\mathbf{P}(\mathbf{r})$ and a corresponding average charge

$$e_{\mathrm{pol}}=-\nabla\cdot\mathbf{P}(\mathbf{r})\ . \tag{2.14}$$

In addition to these charges that can be attributed to the polarization, one also has to consider the charges that result from a wall that runs along the weak bonds. Such a wall alters the charges $m(\mathbf{r})$ in (2.12a). It is easy to see that one has to add to (2.14) fractional charges $e=\pm\frac{1}{2}$ every time a wall starts (or stops) running along weak bonds. At the Ising transition the walls will again melt and large domains will appear. However, since wall portions along the weak bonds cost more energy per bond, the domain wall will contain only short portions with all horizontal parts running along weak bonds. This means that the fractional charges are still confined and combine to integer charges (unless of course $\eta=1$). Therefore, one now has at the Ising transition the following picture for the charges present: (i) There are free *integer* charges that are still in the KT phase at the current temperature. (ii) The charges due to the walls on the strong bonds are given by (2.14) and have the nature of a polarization charge. These charges also contribute, of course, to the screening of the integer charges, resulting in a term in the dielectric constant proportional to $\chi$, where $\chi$ is the susceptibility of the Ising-like system of oriented dipoles. As we shall see in the next section, $\chi$ does not diverge at the Ising critical point, which implies that the Ising transition does not trigger the transition to a Debye-Hückel phase (with $\epsilon^{-1}=0$). This explains the fact that for $\eta\neq 1$ the KT transition can occur within the Ising disordered phase.

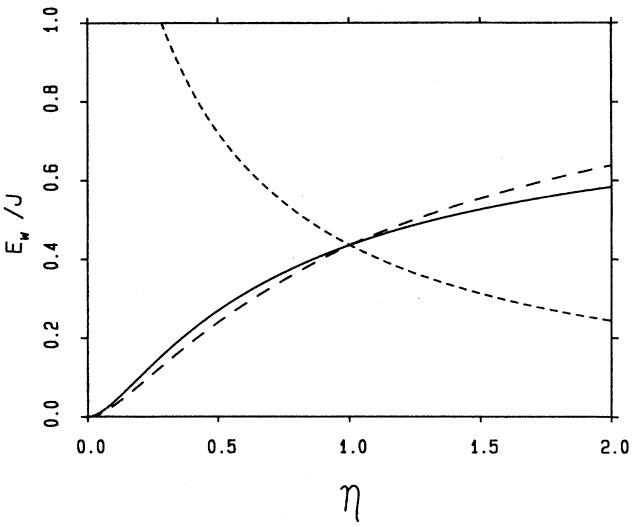


FIG. 3. Energies per unit length of wall for walls in the $x$ direction not on $\eta$ bonds (solid curve), on $\eta$ bonds (short-dashed curve), and for walls in the $y$ direction (long-dashed curve).

## III. THE DIELECTRIC CONSTANT

In this section we will explore the consequences of the newly introduced picture, for the dielectric constant $\epsilon$. To this end we express $\epsilon$ in terms of correlation functions of Coulomb gas quantities in the usual way. For convenience we write the Hamiltonian (2.11) in variables $m'(\mathbf{r})$ and $\mathbf{p}'(\mathbf{r})$ defined by

$$\begin{aligned} m'(\mathbf{r})&=2\pi\sqrt{J}\,m(\mathbf{r})\ ,\\ \mathbf{p}'(\mathbf{r})&=2\pi\sqrt{J}\,\mathbf{p}(\mathbf{r})\ . \end{aligned} \tag{3.1}$$

It follows that

$$H_{CG}=\tfrac{1}{2}\sum_{\mathbf{r},\mathbf{r}'} m'(\mathbf{r})m'(\mathbf{r}')\left[G_0(\mathbf{r}-\mathbf{r}')+\left[\frac{|\eta|}{|\eta|+1}\right]^2\Delta_{yy}G_0(\mathbf{r}-\mathbf{r}')\right]$$
$$-\sum_{\mathbf{r},\mathbf{r}'} m'(\mathbf{r})p_y'(\mathbf{r}')\Delta_y G_0(\mathbf{r}-\mathbf{r}')-\tfrac{1}{2}\sum_{\mathbf{r},\mathbf{r}'} p_y'(\mathbf{r})p_y'(\mathbf{r}')\Delta_{yy}G_0(\mathbf{r}-\mathbf{r}') \ . \tag{3.2}$$

In this calculation only the lowest-order term in the $m'm'$ interaction is of interest. In order to find $\epsilon$ we calculate the screened (sc) potential $G_{sc}$. First we place an infinitesimal charge $\alpha$ at the origin. We can now set up a self-consistent calculation for $G_{sc}$ by writing

$$\alpha G_{sc}(\mathbf{r})=\alpha G_0(\mathbf{r})+\sum_{\mathbf{r}'} G_{sc}(\mathbf{r}-\mathbf{r}')\langle m'(\mathbf{r}')\rangle_\alpha$$
$$-\sum_{\mathbf{r}'}\Delta_y G_{sc}(\mathbf{r}-\mathbf{r}')\langle p_y'(\mathbf{r}')\rangle_\alpha \ , \tag{3.3}$$

where $\langle\ \rangle_\alpha$ denotes a thermal average with respect to the perturbed Hamiltonian. An expansion in terms of correlation functions in the unperturbed system gives, to lowest order in $\alpha$,

$$\langle m'(\mathbf{r}')\rangle_\alpha=-\frac{\alpha}{T}\sum_{\mathbf{r}''} G_0(\mathbf{r}'')\langle m'(\mathbf{r}'')m'(\mathbf{r}')\rangle$$
$$-\frac{\alpha}{T}\sum_{\mathbf{r}''}\Delta_y G_0(\mathbf{r}'')\langle p_y'(\mathbf{r}'')m'(\mathbf{r}')\rangle \ , \tag{3.4a}$$

$$\langle p_y'(\mathbf{r}')\rangle_\alpha=-\frac{\alpha}{T}\sum_{\mathbf{r}''} G_0(\mathbf{r}'')\langle m'(\mathbf{r}'')p_y'(\mathbf{r}')\rangle$$
$$-\frac{\alpha}{T}\sum_{\mathbf{r}''}\Delta_y G_0(\mathbf{r}'')\langle p_y'(\mathbf{r}'')p_y'(\mathbf{r}')\rangle \ . \tag{3.4b}$$

We insert (3.4) in (3.3) and perform a Fourier transformation with respect to sublattice 1 [the Fourier transformed with respect to sublattice $i$ (the entire lattice) has superscript $i$ (no superscript)]. It follows that

$$\hat{\mathbf{G}}^{\,1}_{SC}(\mathbf{k})=\hat{\mathbf{G}}^{\,1}_{0}(\mathbf{k})+\frac{\hat{\mathbf{G}}^{\,1}_{SC}(\mathbf{k})\hat{\mathbf{G}}^{\,1}_{0}(\mathbf{k})}{T}$$
$$\times[-\hat{\mathbf{g}}^{\,1}_{mm}(\mathbf{k})+2i\sin k_y\hat{\mathbf{g}}^{\,1}_{pm}(\mathbf{k})$$
$$-\sin^2 k_y\hat{\mathbf{g}}^{\,1}_{pp}(\mathbf{k})] \ , \tag{3.5}$$

where $g_{pm}(\mathbf{r})=\langle p_y'(\mathbf{0})m'(\mathbf{r})\rangle$, etc. If we define

$$\mathbf{k}_*=\left[k_x,\left[\frac{2}{|\eta|+1}\right]^{1/2}k_y\right]$$

then we have

$$\hat{\mathbf{G}}^{\,1}_{0}(\mathbf{k})=\frac{1}{2k_*^2} \text{ if } |\mathbf{k}_*|\ll 1 \ . \tag{3.6}$$

Using this we obtain from (3.5) for small $|\mathbf{k}_*|$

$$\hat{\epsilon}^{\,1}(\mathbf{k})\equiv\frac{\hat{\mathbf{G}}^{\,1}_{0}(\mathbf{k})}{\hat{\mathbf{G}}^{\,1}_{sc}(\mathbf{k})}\simeq 1+\frac{1}{2k_*^2T}[\hat{\mathbf{g}}^{\,1}_{mm}(\mathbf{k})-2ik_y\hat{\mathbf{g}}^{\,1}_{pm}(\mathbf{k})+k_y^2\hat{\mathbf{g}}^{\,1}_{pp}(\mathbf{k})]$$
$$\simeq 1-\frac{1}{4k_*^2T}\sum_{\mathbf{r}}\langle m'(\mathbf{0})m'(\mathbf{r})\rangle(\mathbf{k}\cdot\mathbf{r})^2+\frac{k_y}{k_*^2T}\sum_{\mathbf{r}}\langle p_y'(\mathbf{0})m'(\mathbf{r})\rangle(\mathbf{k}\cdot\mathbf{r})+\frac{k_y^2}{2k_*^2T}\sum_{\mathbf{r}}\langle p_y'(\mathbf{0})p_y'(\mathbf{r})\rangle \ . \tag{3.7}$$

We can now find the dielectric constant $\epsilon$ by taking the limit $|\mathbf{k}|\to 0$. Here the dielectric constant will be anisotropic and we must use the tensor $\epsilon_{ij}$ $(i,j=x,y)$. The diagonal elements can be found by

$$\epsilon_{xx}=\lim_{k_x\to 0}\hat{\epsilon}^{\,1}(k_x,0)$$

and (3.8)

$$\epsilon_{yy}=\lim_{k_y\to 0}\hat{\epsilon}^{\,1}(0,k_y) \ .$$

The resulting formula expresses the well-known fact that the change in the dielectric constant can be expressed in the fluctuation of the polarization. In the present picture this involves a sum of the polarization $\mathbf{P}'=(2/N)\sum_{\mathbf{r}}\mathbf{p}'(\mathbf{r})$ due to the dipoles of the shifted charges and the polarization

$$\mathbf{P}_{free}=\frac{2}{N}\sum_{\mathbf{r}} m'(\mathbf{r})\mathbf{r}$$

due to the free charges. Since the length of $\mathbf{p}'$ is fixed (to $2\pi\sqrt{J}\,[|\eta|/(|\eta|+1)]$, the maximum length of the polarization $\mathbf{P}'$ is also fixed. However, the length of $\mathbf{P}_{free}$ can increase and will in fact diverge at the KT transition of the unit charges. Presently we are interested in a temperature regime where the unit charges are still (logarithmically) bound and consequently $|\mathbf{P}_{free}|$ is finite. If we further assume that the density of $m'$ charges is small (which means that $\eta$ is chosen such that there is an appreciable energy difference between walls on weak and strong bonds) than we can approximate (3.7) by only considering the contribution of the last term. From (3.7) we then find with (3.8)

$$\epsilon_{xx}=1 \ ,$$
$$\epsilon_{yy}=1+\pi^2\frac{J}{T}\frac{\eta^2}{|\eta|+1}\sum_{\mathbf{r}}\langle s(\mathbf{0})s(\mathbf{r})\rangle \ . \tag{3.9}$$

Relations (3.1) and (2.12b) have been used to retrieve the

original $s$ variables. From (3.9) we see that, if there is an important activity in the dipoles $s$ at a low density of $m$ charges, then this will affect only $\epsilon_{yy}$ and not $\epsilon_{xx}$. Note that $\epsilon_{yy}$ contains a susceptibility of a system with an Ising symmetry. We define the $\mathbf{k}$-dependent susceptibility as

$$\hat{\chi}(\mathbf{k})=\sum_{\mathbf{r}} e^{i\mathbf{k}\cdot\mathbf{r}}[e^{-i\pi x}\langle s(\mathbf{0})s(\mathbf{r})\rangle-\langle s(\mathbf{0})\rangle^2] \tag{3.10}$$

since $e^{-i\pi x}s(\mathbf{r})$ is the order parameter of the system (compare the ground-state structure). Then (3.9) becomes

$$\epsilon_{yy}=1+\pi^2\frac{J}{T}\frac{\eta^2}{|\eta|+1}\hat{\chi}(\pi,0)\ . \tag{3.11}$$

Since this equation involves the $\mathbf{k}\neq\mathbf{0}$ susceptibility of the Ising model, there is *no* divergence of the dielectric constant at the Ising critical point. In the pure nearest-neighbor Ising model, $\hat{\chi}(\pi,0)$ has a $t\ln|t|$ ($t=1-T/T_c$) anomaly.[16] Here, one expects $\epsilon_{yy}$ to have the same anomaly, although there might be a modification due to the long-range dipolar interaction. It is remarkable that Granato and Kosterlitz[13] were led to the same conclusion, along completely different lines of reasoning.

The diagonal elements of the $\epsilon$ tensor are related to the helicity moduli $\gamma_x$ and $\gamma_y$ of the cosine model. With the usual definition[17] and (1.1) we easily find that for this model

$$\gamma_i=\frac{1}{N}\left[\left\langle\sum_{\mathbf{r}}|J_{\mathbf{r},\mathbf{r}+\hat{\mathbf{e}}_i}|\cos[\theta(\mathbf{r})-\theta(\mathbf{r}+\hat{\mathbf{e}}_i)-2\pi A(\mathbf{r},\mathbf{r}+\hat{\mathbf{e}}_i)]\right\rangle\right.$$
$$\left.-\frac{1}{k_BT}\left\langle\left[\sum_{\mathbf{r}}|J_{\mathbf{r},\mathbf{r}+\hat{\mathbf{e}}_i}|\sin[\theta(\mathbf{r})-\theta(\mathbf{r}+\hat{\mathbf{e}}_i)-2\pi A(\mathbf{r},\mathbf{r}+\hat{\mathbf{e}}_i)]\right]^2\right\rangle\right], \tag{3.12}$$

where $i=x,y$ and $N$ is the number of sites in the system.

Comparing (3.8) with its analog in Ref. 17, we see that there is a qualitative correspondence

$$\gamma_x\sim\epsilon_{yy}^{-1}$$
and (3.13)
$$\gamma_y\sim\epsilon_{xx}^{-1}\ .$$

The correspondence is, of course, not exact because the two models (cosine and periodic Gaussian) are not the same but only chosen such that they are expected to describe the same physics. On the basis of the present analysis of the periodic Gaussian model one would expect that a numerical analysis of the cosine model should exhibit the following features: (i) A low-temperature Ising-like transition characterized by a divergence of $\hat{\chi}(\mathbf{k}=0)$. The helicity modulus at this transition point should remain finite, but its temperature derivative should show a $\ln|t|$ divergence due to the $t\ln|t|$ term in $\hat{\chi}(k_x=\pi,k_y=0)$. (ii) This transition is followed by a KT transition at a higher temperature, where the integer charges are no longer logarithmically bound.

## IV. NUMERICAL RESULTS

In this section we study some important features of the low-temperature behavior of the cosine model at $\eta=0.5$ by Monte Carlo (MC) simulations and show that we can understand them with the ideas of Sec. II. The MC simulations were performed using the standard Metropolis algorithm. Typically three or four independent runs were made, with 15 000 to 20 000 measurements each, after 5000 configurations were discarded for thermalization. We determined for each spin configuration the corresponding charge configuration with

$$M(\mathbf{R})=\tfrac{1}{2}\mathrm{sign}\left[\sum(|J_{\mathbf{r}\mathbf{r}'}|/J)\sin[\theta(\mathbf{r})-\theta(\mathbf{r}')-2\pi A(\mathbf{r},\mathbf{r}')]\right]. \tag{4.1}$$

The summation is over four bonds surrounding $\mathbf{R}$. In this way several quantities related to the charges can be calculated.

It is interesting to study the proliferation of domain walls at the low-temperature phase transition. Therefore, we evaluated the number of wall segments per bond available for three different types of walls. (Note that vertical wall segments have twice as many bonds available as the horizontal types.) These densities can be written as

$$D_{\mathrm{SH}}=\tfrac{1}{2}+2\langle M(\mathbf{0})M(\hat{\mathbf{e}}_y)\rangle\ ,$$
$$D_{\mathrm{WH}}=\tfrac{1}{2}+2\langle M(\mathbf{0})M(-\hat{\mathbf{e}}_y)\rangle\ , \tag{4.2}$$
$$D_V=\tfrac{1}{2}+2\langle M(\mathbf{0})M(\hat{\mathbf{e}}_x)\rangle\ ,$$

for wall segments on strong horizontal (SH), weak horizontal (WH), and vertical ($V$) bonds, respectively. The MC data are plotted in Fig. 4. There are two transition points. It is clearly visible that there is a sudden proliferation of walls at the low-temperature transition and this proliferation does not involve walls on the weak bonds. This result thus supports the idea that the low-temperature transition is an Ising transition in the system of dipoles and that the $m$ charges hardly take part in this transition.

A clear manifestation of the role of the dipoles $s(\mathbf{r})$ as Ising variables is in the behavior of the ferromagnetic susceptibility $\hat{\chi}(0,0)$. In the pure Ising model we have

$$\hat{\chi}^{\mathrm{Ising}}(0,0)\sim|t|^{-7/4}\ \text{ as } t\to0\ , \tag{4.3}$$

with $t=1-(T/T_c)$. As discussed in Ref. 18, we have for a system with linear size $L$,

$$\hat{\chi}_L^{\mathrm{Ising}}(0,0)\cong L^{7/4}f[L(T-T_c)]\ , \tag{4.4}$$

where $f$ is some function which is finite at $t=0$ and independent of $L$ (if $L$ is not too small). We evaluated $\hat{\chi}_L(0,0)$ using the charge distribution obtained with (4.1). Then we plotted $\hat{\chi}_L(0,0)L^{-7/4}$ as a function of $(T-T_c)L$ and varied $T_c$ (the transition temperature of the *infinite*

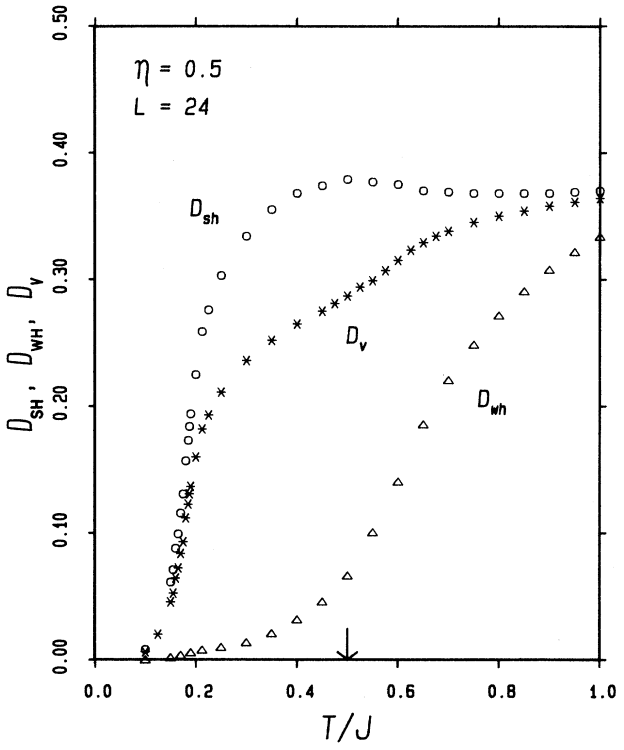


FIG. 4. Number of bonds-in-walls per bond available for weak horizontal (WH), strong horizontal (SH), and vertical bonds ($v$) [see (4.2)]. The arrow indicates the approximate location of the high-temperature phase transition.

system) to optimize the data "collapse" (see Fig. 5). The transition temperature found in this way is $T_c=0.175$, which is in agreement with specific-heat data (not presented here). We see that, away from the transition temperature $T_{c,L}$ of the finite system, the peaks indeed merge. The error bars indicate that it is difficult to determine $\hat{\chi}_L(0,0)$ in the neighborhood of $T_{c,L}$. This is why

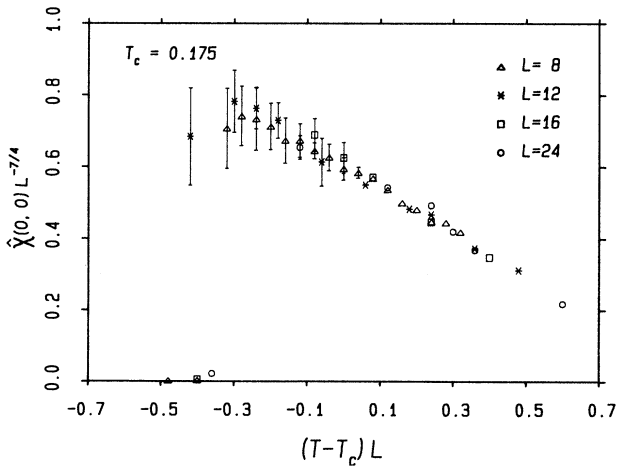


FIG. 5. Rescaled ferromagnetic susceptibility as a function of a rescaled temperature for lattices with different linear size $L$. The scale factors are obtained from the pure 2D Ising model.

we used this method instead of a peak height analysis. From Fig. 5 we conclude that the dipoles indeed behave as Ising variables and that the long-range part of the interaction does not modify the critical exponent drastically.

As mentioned in the previous section, we obtain insight in $\epsilon_{xx}$ and $\epsilon_{yy}$ numerically by monitoring the helicity moduli $\gamma_x$ and $\gamma_y$. We computed $\gamma_x$ and $\gamma_y$ using relation (3.12). The MC data are shown in Fig. 6 (see also, Ref. 19). The asymptotic values of $\gamma_x(T)$ and $\gamma_y(T)$ as $T\rightarrow 0$ should equal the "bare" spin-wave stiffness of the cosine model for a spin wave in the $x$ resp. $y$ direction. Given the ground state of the model[4] and (3.12) it is easy to calculate that for $\eta>\frac{1}{3}$,

$$\gamma_x(T=0)=J\frac{\eta}{2}\sqrt{(\eta+1)/\eta}$$

and

$$\gamma_y(T=0)=J\tfrac{1}{2}\sqrt{(\eta+1)/\eta}$$

in accordance with the numerical findings for $\eta=\frac{1}{2}$. The low-temperature transition is visible as a kink in $\gamma_x$ and the effect on $\gamma_y$ is very small. This is just the behavior expected from (3.9) and (3.13). We have discussed that $d\gamma_x/dT$ should show a $\ln|t|$ divergence at this transition point. In extension of the work of Granato and Kosterlitz,[13] for larger lattices and with the inclusion of error

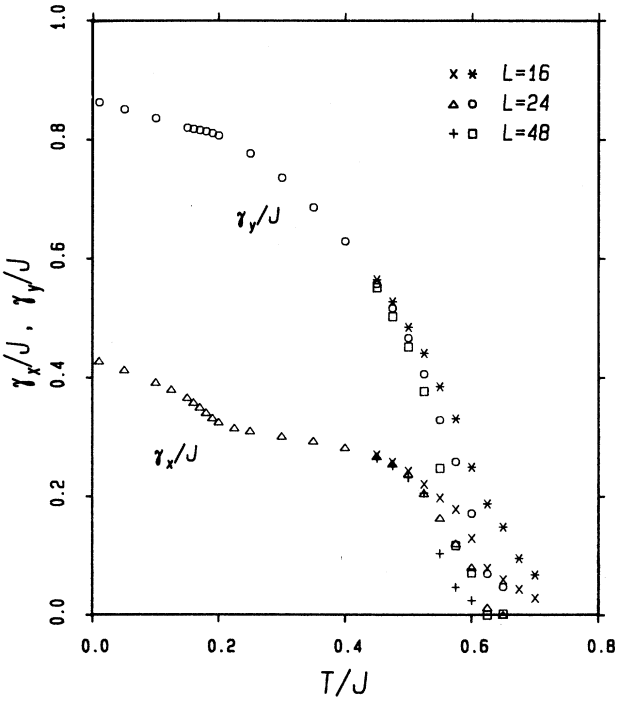


FIG. 6. Helicity modulus in $x$ and $y$ direction for $\eta=0.5$ and for different lattices. The size dependence is only appreciable near the high-temperature phase transition.

bars, we calculated $\frac{1}{2}(d/d\beta)(\beta\gamma_x)$ using

$$\frac{1}{2}\frac{d}{d\beta}(\beta\gamma_x)=\frac{U_a-U_p}{\pi^2} . \tag{4.5}$$

Here, $U_p(U_a)$ is the total internal energy calculated with periodic (antiperiodic) boundary conditions along the $x$ direction. This equation is, strictly speaking, only valid for an infinite system because only in that case is the twist per spin $\pi/L$ really infinitesimal. The right-hand side of (4.5) was calculated for different lattice sizes. The result is plotted in Fig. 7. In the inset we plotted the peak height as a function of $\ln(L)$. In the critical region both $U_p$ and $U_a$ were determined using at least three independent runs of 30 000 to 40 000 measurements each, after discarding 10 000 configurations for thermalization. In spite of this, the results for larger lattices are not very accurate. However, they are consistent with the expected linear relation between the peak height and $\ln(L)$.

The high-temperature phase transition clearly exhibits the KT-like behavior, assumed by Berge *et al.*,[4] who conjectured this transition on the basis of specific-heat data only. To determine the size of the "universal" jump at the KT transition[20] one must realize that the present model is highly anisotropic. The bare couplings in $x$ and $y$ direction are different to begin with (a factor $\frac{1}{2}$ in the present case, see above) but also renormalize in a different way mainly due to the anisotropic system of bound dipoles. For finite temperatures one arrives at effectively (renormalized) Gaussian couplings $\gamma_x(T)$ and $\gamma_y(T)$ with a nonuniversal renormalized ratio $\alpha_r^2(T)=[\gamma_x(T)/\gamma_y(T)]$. The universal jump, in this case, is expected for the geometric mean

$$\gamma(T)=\sqrt{\gamma_x\gamma_y}=\alpha_r(T)\gamma_y(T) .$$

[This can be seen by a rescaling of one of the axes of the Gaussian model, compare Eq. (2.10).] Figure 8 shows a plot of $(\gamma_x\gamma_y)^{1/2}/J$ versus $T/J$. The drop in the helicity modulus is seen to be consistent with the universal jump $(2T/\pi J)$. This supports the idea that the high-temperature transition is a normal KT transition in the Coulomb gas of integer charges.

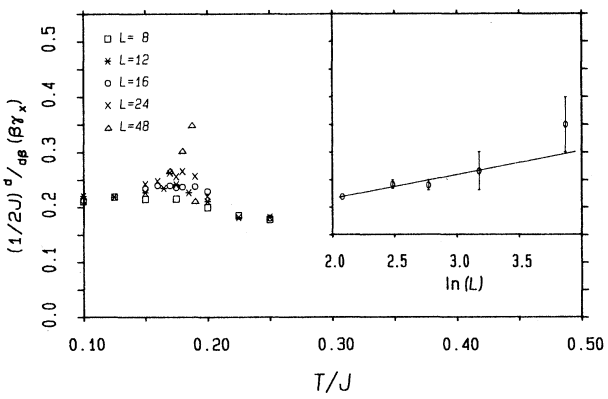


FIG. 7. Temperature dependence of $(1/2J)(d/d\beta)(\beta\gamma_x)$ for different lattices. The size dependence of the peak height is shown in the inset.

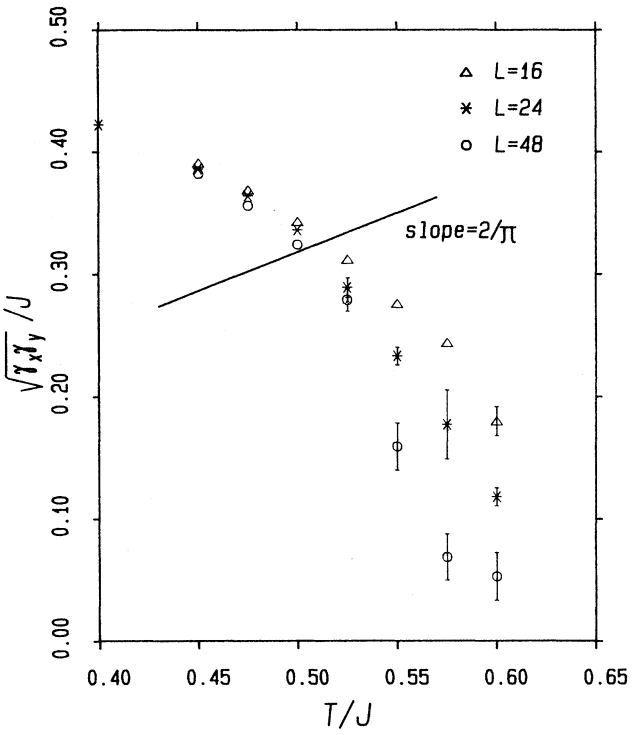


FIG. 8. Temperature and size dependence of $(\gamma_x\gamma_y)^{1/2}/J$ for temperatures around the high-temperature phase transition. The solid line is the universal jump prediction.

## V. CONCLUSION

In this paper we have made a study of uniformly frustrated $XY$ models with an inhomogeneous coupling distribution. It was argued via a Coulomb gas picture that the formation of dipoles with a fixed length, would alter the phase-transition mechanism in such a way that the Ising transition would not automatically liberate fractional charges causing a KT transition to occur at the same time. A further consequence of this picture is the prediction that the dielectric constant (or inverse helicity modulus) should not diverge at the Ising critical point. Instead it will contain an "energy-like" anomaly. The divergence of the dielectric constant is expected at a higher temperature where the integer charges are no longer confined by the Coulomb interaction. These predictions are confirmed by a Monte Carlo simulation of a frustrated $XY$ model with weak and strong bonds at a strength ratio $\eta=\frac{1}{2}$. We would expect that the fractional charges remain confined at the Ising transition for $\eta$ approaching unity. The reason is that free fractional charges require a domain wall to run along many energetically unfavorable bonds. Thus, even a small energy difference (as is the case for $\eta\simeq 1$) will result in a vanishing Boltzman weight. Therefore, the Ising transition will not induce the KT transition by a fractional charge mechanism for $\eta\neq 1$. However, it might happen that the renormalization of the dielectric constant by the Ising susceptibility $\chi$ will precipitate the KT transition. The

fact that $\chi$ is a continuous function of the parameters ($\eta$ and $T$) implies that this effect can only result in a *shift* of the point at which the KT transition and the Ising transition coincide. Since there is ample evidence that this point is located at $\eta=1$ (Refs. 6–8, 10, and 12) we expect (using the symmetry $\eta\leftrightarrow\eta^{-1}$) that $T_{\rm Ising}(\eta)<T_{\rm KT}(\eta)$ for all $\eta\neq1$; the transitions only coincide at $\eta=1$. Monte Carlo data available[4] seem to support this, but are, as yet, not conclusive. One needs more and better Monte Carlo data for larger lattices in order to separate the transitions as $\eta$ approaches unity.

## ACKNOWLEDGMENTS

One of us (J.v.H.) is grateful to R. J. Silbey for the opportunity to spend a year at Massachusetts Institute of Technology (MIT), where part of this work was performed; H.E. thanks him for his hospitality during visits to MIT. This work was partially supported by the Dutch Organization for the Advancement of Pure Science (F.O.M.).

## APPENDIX

We derive the exact expression for (the Fourier transform of) $G$ as determined by (2.3) and (2.4). Without loss of generality we can write

$$G(\mathbf{R}'',\mathbf{R}')=G_{ij}(\mathbf{R}''-\mathbf{R}') \quad (i,j=1,2) , \tag{A1}$$

when $\mathbf{R}''$ is on sublattice $i$ and $\mathbf{R}'$ on sublattice $j$. Furthermore, we define the operators

$$\begin{aligned} d_x f(\mathbf{R})&=\left[\frac{|\eta|+1}{|\eta|}-\Delta_{xx}\right]f(\mathbf{R}) ,\\ d_y f(\mathbf{R})&=\frac{1}{|\eta|}f(\mathbf{R}-\hat{\mathbf{e}}_2)+f(\mathbf{R}+\hat{\mathbf{e}}_2) ,\\ d_y^{+} f(\mathbf{R})&=\frac{1}{|\eta|}f(\mathbf{R}+\hat{\mathbf{e}}_2)+f(\mathbf{R}-\hat{\mathbf{e}}_2) . \end{aligned} \tag{A2}$$

Substituting (A1) in (2.3) we find

$$\begin{aligned} d_x G_{11}(\mathbf{R}_1)-d_y G_{21}(\mathbf{R}_1)&=\delta_{\mathbf{R}_1,0} ,\\ d_x G_{12}(\mathbf{R}_2)-d_y G_{22}(\mathbf{R}_2)&=0 ,\\ d_x G_{21}(\mathbf{R}_2)-d_y^{+} G_{11}(\mathbf{R}_2)&=0 ,\\ d_x G_{22}(\mathbf{R}_1)-d_y^{+} G_{12}(\mathbf{R}_1)&=\delta_{\mathbf{R}_1,0} , \end{aligned} \tag{A3}$$

where $\mathbf{R}_1$ and $\mathbf{R}_2$ denote arbitrary sites on lattices 1 and 2, respectively. A Fourier transform with respect to the relevant sublattice gives

$$\begin{aligned} \hat{\mathbf{G}}^{1}_{11}(\mathbf{k})&=\hat{\mathbf{G}}^{1}_{22}(\mathbf{k})=\frac{\hat{\mathbf{d}}_x(\mathbf{k})}{|\hat{\mathbf{d}}_x(\mathbf{k})|^2-|\hat{\mathbf{d}}_y(\mathbf{k})|^2} ,\\ \hat{\mathbf{G}}^{2}_{12}(\mathbf{k})&=\hat{\mathbf{G}}^{2*}_{21}(\mathbf{k})=\frac{\hat{\mathbf{d}}_y(\mathbf{k})}{|\hat{\mathbf{d}}_x(\mathbf{k})|^2-|\hat{\mathbf{d}}_y(\mathbf{k})|^2} , \end{aligned} \tag{A4}$$

where

$$\hat{\mathbf{d}}_x(\mathbf{k})=\frac{|\eta|+1}{|\eta|}+2(1-\cos k_x)$$

and

$$\hat{\mathbf{d}}_y(\mathbf{k})=\frac{1}{|\eta|}e^{+ik_y}+e^{-ik_y} . \tag{A5}$$

The $*$ denotes complex conjugation.

To obtain the $G_0$ of Sec. II, we note that $G_{ij}$ will be determined largely by the dominant terms in the Taylor expansion of $\hat{\mathbf{G}}_{ij}$ in the neighborhood of the origin. Now

$$|\hat{\mathbf{d}}_x(\mathbf{k})|^2-|\hat{\mathbf{d}}_y(\mathbf{k})|^2=\frac{(|\eta|+1)^2}{4|\eta|}\times[\hat{\mathbf{G}}_0^{-1}(\mathbf{k})\hat{\mathbf{G}}_0^{-1}(\tilde{\mathbf{k}})-r(\mathbf{k})] ,$$

where

$$r(\mathbf{k})=4\left[\frac{|\eta|-1}{|\eta|+1}\right]^2(1-\cos k_x)^2=O(|\mathbf{k}|^4)(|\mathbf{k}|\to0)$$

and

$$\tilde{\mathbf{k}}=(k_x,k_y-\pi) .$$

If we neglect $r(\mathbf{k})$ we find that

$$G_{11}(\mathbf{R}_1)\simeq\frac{2}{N}\sum_{\mathbf{k}\in B'}\frac{4|\eta|}{(|\eta|+1)^2}\hat{\mathbf{d}}_x(\mathbf{k})\hat{\mathbf{G}}_0(\mathbf{k})\hat{\mathbf{G}}_0(\tilde{\mathbf{k}})e^{-i\mathbf{k}\cdot\mathbf{R}_1}=\frac{1}{N}\sum_{\mathbf{k}\in B}\frac{8|\eta|}{(|\eta|+1)^2}\times\left[\frac{\hat{\mathbf{d}}_x(\mathbf{k})}{\hat{\mathbf{G}}_0^{-1}(\mathbf{k})+\hat{\mathbf{G}}_0^{-1}(\tilde{\mathbf{k}})}\right]\hat{\mathbf{G}}_0(\mathbf{k})e^{-i\mathbf{k}\cdot\mathbf{R}_1}\simeq G_0(\mathbf{R}_1) ,$$

where $B$ and $B'$ refer to the Brillouin zone corresponding to the entire lattice and one sublattice, respectively. The other cases follow in a similar manner.

With the use of a Fourier transform it is straightforward to calculate the energy per unit length of an infinite straight domain wall. The result for vertical walls is

$$E_{w,v}=-2\pi^2 J\int_{-\pi}^{\pi}\frac{dk_x}{2\pi}\frac{1}{1+e^{ik_x}}i\frac{\partial}{\partial k_x}[\hat{\mathbf{G}}^{1}_{11}(k_x,0)-\mathrm{Re}\hat{\mathbf{G}}^{2}_{12}(k_x,0)] .$$

For the two types of horizontal walls we find

$$E_{w,h} = -2\pi^2 J \int_{-\pi/2}^{\pi/2} \frac{dk_y}{\pi} \frac{1}{1-e^{2ik_y}} i \left[ \frac{\partial}{\partial k_y} \hat{\mathbf{G}}^{1}_{11}(\pi, k_y) - e^{ik_y} \frac{\partial}{\partial k_y} \mathrm{Re}\hat{\mathbf{G}}^{2}_{12}(\pi, k_y) \pm e^{ik_y} \mathrm{Im}\hat{\mathbf{G}}^{2}_{12}(\pi, k_y) \right],$$

where the $+(-)$ sign applies for walls on $\eta$ bonds (not on $\eta$ bonds). The expressions have been evaluated numerically and the result is given in Fig. 3.


[1]For a recent review of the field see Physica **152B**, 1 (1988).
[2]P. Martinoli, Physica **152B**, 146 (1988).
[3]D. Van Harlingen (unpublished).
[4]B. Berge, H. T. Diep, A. Ghazali, and P. Lallemand, Phys. Rev. B **34**, 3177 (1986).
[5]H. van der Zant and J. E. Mooij (private communication).
[6]S. Teitel and C. Jayaprakash, Phys. Rev. B **27**, 598 (1983).
[7]T. C. Halsey, J. Phys. C **18**, 2437 (1985).
[8]D. H. Lee, J. D. Joannopoulos, J. W. Negele, and D. P. Landau, Phys. Rev. B **33**, 450 (1986), and references therein.
[9]E. Granato and J. M. Kosterlitz, J. Phys. C **19**, L59 (1986); E. Granato, J. M. Kosterlitz, and J. Poulter, Phys. Rev. B **33**, 4767 (1986).
[10]J. E. Van Himbergen, Phys. Rev. B **33**, 7857 (1986); **34**, 6567 (1986), and references therein.
[11]S. E. Korshunov, J. Stat. Phys. **43**, 17 (1986).
[12]J. M. Thijssen and H. J. F. Knops, Phys. Rev. B **37**, 7738 (1988).
[13]E. Granato and J. M. Kosterlitz (unpublished).
[14]L. P. Kadanoff, J. Phys. A **11**, 1399 (1978).
[15]J. Villain, J. Phys. (Paris) **36**, 581 (1975).
[16]M. F. Sykes and M. E. Fisher, Phys. Rev. Lett. **1**, 321 (1958); Physica **28**, 919 (1962).
[17]T. Ohta and J. D. Jasnow, Phys. Rev. B **20**, 139 (1979).
[18]K. Binder, in *Monte Carlo Methods in Statistical Physics* (Springer-Verlag, Berlin, 1979), Sec. 1.2.6.
[19]J. E. Van Himbergen, Physica **152B**, 46 (1988).
[20]J. M. Kosterlitz, J. Phys. C **7**, 1046 (1974); J. Jose, L. P. Kadanoff, S. Kirkpatrick, and D. R. Nelson, Phys. Rev. B **16**, 1217 (1977).